Infection and Drug Resistance

Dovepress
Taylor & Francis Group

Open Access Full Text Article

ORIGINAL RESEARCH

# Phage vB_Kpn_HF0522: Isolation, Characterization, and Therapeutic Potential in Combatting K1 *Klebsiella pneumoniae* Infections

Tao Yan[1,2], Qiuyan Wang[2], Chengcheng Ma[2], Xuan Teng[2], Zhen Gong[2], Wenwen Chu[2], Qiang Zhou[2], Zhou Liu[1]

[1]Department of Clinical Laboratory Center, Anhui Chest Hospital, Hefei, 230031, People's Republic of China; [2]Department of Clinical Laboratory, the Second Affiliated Hospital of Anhui Medical University, Hefei, 230601, People's Republic of China

Correspondence: Zhou Liu, Department of Clinical Laboratory Center, Anhui Chest Hospital, Hefei, People's Republic of China, Email liuzhou0112@ahmu.edu.cn



**Purpose:** *Klebsiella pneumoniae* is a globally prevalent pathogen responsible for severe hospital- and community-acquired infections, and presents significant challenges for clinical management. Current therapeutic strategies are no longer able to meet the clinical needs; therefore, there is an urgent need to develop novel therapeutic strategies. This study aimed to evaluate the efficacy of phage therapy in treating bacterial infections.

**Methods:** Isolated phage vB_Kpn_HF0522 and phage morphology were observed using transmission electron microscopy. Analysis of vB_Kpn_HF0522 characteristics, including optimal multiplicity of infection (MOI), one-step growth curve, host range, stability in different environments, and adsorption capacity. The phage genomic sequence was analyzed to explore evolutionary relationships. The effect of phage vB_Kpn_HF0522 on biofilms was assessed using crystal violet staining assay. The *Galleria mellonella* (*G. mellonella*) infection model and mouse infection models were established to evaluate the practical application potential of the phage and the fitness cost of phage-resistant bacteria.

**Results:** Phage was isolated from hospital sewage for experimental studies. Genome analysis revealed that vB_Kpn_HF0522 is a double-stranded linear DNA virus. Biological characterization demonstrated that this phage specifically targets serotype K1 *K. pneumoniae* with an optimal multiplicity of infection (MOI) of 0.01, effectively disrupting biofilms and inhibiting bacterial growth. The bacterial growth rate remained largely unchanged after the phage resistance mutation, but mice infected with the mutant strain showed significantly higher survival rates than those infected with the wild-type strain. vB_Kpn_HF0522 increased the survival rate of infected *G. mellonella* from 12.5% to 75%, inhibited incisional surgical site infections and alleviated inflammatory response in mice.

**Conclusion:** These findings indicate that vB_Kpn_HF0522 has significant potential for treating specific bacterial infections, and may serve as an antimicrobial agent for research and clinical anti-infective therapy.

**Keywords:** phage vB_Kpn_HF0522, phage therapy, *Klebsiella pneumoniae*, phage resistance, incisional surgical site infection, biofilm

## Introduction

*K. pneumoniae* is widely distributed in the environment and is a typical opportunistic pathogen. *K. pneumoniae* can cause infections in some parts of the body, such as the lungs, abdominal cavity, urinary tract, bones, muscles, skin, and soft tissues, and some strains can lead to primary bacteremia in healthy people.[1–3] In recent years, there has been an increase in the detection rate of multidrug-resistant *Klebsiella pneumoniae* (MDR-KP), which further limits the effectiveness of existing antimicrobial agents and complicates treatment efforts.[4,5] A key cause of *K. pneumoniae* pathogenicity is its capsular polysaccharide (CPS), which allows it to evade the host immune system and hinders the penetration of antibacterial drugs.[6,7] One of the most prevalent serotypes among *K. pneumoniae* is the K1 capsular type, exhibiting stronger resistance to phagocytosis by macrophages and greater resistance to extracellular and intracellular killing by

Received: 6 November 2024
Accepted: 17 January 2025
Published: 10 February 2025

neutrophils, thus facilitating systemic dissemination, and its wide spread has become a significant public health issue.[8–12] Antibiotic therapy is commonly used to treat bacterial infections, but treatment can still fail even when the bacteria are sensitive to antibiotics. Studies have shown that factors such as biofilm formation, patient immunocompromise, insufficient drug penetration at the site of infection, and bacterial retention may all contribute to poor treatment outcome.[13–16] As a result, pure antibiotic therapies are no longer sufficient to meet clinical demands, emphasizing the pressing need for innovative antimicrobial approaches.

Bacteriophages (phages) are viruses that selectively target bacteria, and some phages recognize and induce host bacterial death without disturbing the normal microbiota.[17–19] A clinical case report indicated that compared with systemic antibiotic treatment, bacteriophage treatment caused minimal damage to the patient's gut microbiota.[20] Given their abundance in nature, potent antimicrobial capacity, and low toxicity to humans, phages show potential as a viable alternative or adjunct therapy to antibiotics, enhancing anti-infection treatments.[21,22] Current studies have confirmed the efficacy of phages in eliminating K1 *K. pneumoniae*, with some findings showing that phages can significantly improve the survival rates of infected mice or *Galleria mellonella* (*G. mellonella*).[22–25] However, research on the therapeutic potential of phages in treating surgical wound infections remains limited. The development of novel phages can enable personalized treatments and provide an effective strategy to manage the emergence of phage-resistant bacteria.[26]

Numerous clinical studies have demonstrated the excellent potential of phages in infection. For instance, in 2019, Saskia Kuipers et al reported phage therapy for chronic recurrent urinary tract infection in a kidney transplant patient.[27] In 2021, Apurva Virmani Johri et al documented successful phage therapy for chronic bacterial prostatitis in which multiple antibiotic treatments failed.[28] In 2022, Anaïs Eskenazi et al reported a case in which phage therapy combined with antibiotics successfully treated a fracture-related infection caused by antibiotic-resistant *K. pneumoniae*.[29] These cases offer empirical evidence supporting the utilization of phage therapy as an alternative treatment approach for bacterial infections. Some countries and regions have established clear guidelines and standards for phage therapies. For example, the European Union and the United States require phage production to adhere to Good Manufacturing Practice (GMP) standards to ensure the quality and safety of phage products.[30] It is believed that with the continuous advancement of biotechnology and the deepening of phage research, phage therapy will become an even more important part of anti-infective therapy in the future.

In this study, we isolated a phage capable of lysing the K1 *K. pneumoniae* strain from hospital sewage, named vB_Kpn_HF0522. According to genomic analysis, this phage is a double-stranded DNA virus that belongs to the genus Drulisvirus. To characterize its biological traits, we investigated its one-step growth curve, adsorption onto host bacteria, and its environmental resilience. Using a crystal violet staining assay, we assessed their ability to inhibit or disrupt bacterial biofilms. We also isolated phage-resistant mutant bacteria and examined whether these mutations affected the efficacy of phage therapy using a mouse infection model. Additionally, by monitoring the bacterial growth curves and survival rate of infected *G. mellonella*, we studied the ability of the phage to lyse bacteria both in vitro and in vivo.

Surgical site infection (SSI), caused by bacterial invasion through surgical incisions, threatens the lives of patients and is a highly prevalent healthcare-associated infection (HAI) worldwide.[31,32] Research has examined the efficacy of phage therapy for wound infections, however, studies on the treatment of incisional surgical site infections remain limited.[33–35] Therefore, we established a mouse incisional surgical site infection model to simulate human surgical wound infection and healing processes and evaluated the application potential of vB_Kpn_HF0522. In conclusion, we discovered and characterized phage vB_Kpn_HF0522, investigated its genetic information and biological features, and verified its effects on host bacteria in vivo and in vitro.

# Materials and Methods

## Animals

All animals used in this study were reviewed and approved by the Institutional Animal Care and Use Committee of Anhui Medical University (approval number LLSC20240703), and all experiments were performed in accordance with the guidelines. 6–8-week-old female BALB/c mice purchased from Henan Skbex Biotechnology Co., Ltd. (Anyang,

China) were selected for the study. The mice were housed under specific pathogen-free conditions with free access to food and water that did not contain antibacterial agents.

## Isolation and Identification of Bacteria

The bacterial strains used in this study were derived from clinical diagnostic samples routinely stored in the Department of Clinical Laboratory at the Second Affiliated Hospital of Anhui Medical University. The study was approved by the ethics committee of the hospital (approval number KYLL20240200). The bacterial species were identified using a Microflex LT mass spectrometer (Bruker Corporation, Germany). The DNA of the strains was amplified using wzi type primers (forward: 5′-GTGCCGCGAGCGCTTTCTATCTTGGTATTCC-3′; reverse: 5′-GAGAGCCACTGGTTCCAGAATTACCGC-3′) and the PCR products were sequenced by Sangon Biotech Co., Ltd. (Shanghai, China). The wzi type and the corresponding capsular serotype were identified using a database (https://bigsdb.Pasteur.fr/klebsiella/).[36]

## Phage Isolation and Purification

Isolation and purification of bacteriophages followed the methods described in previous studies, with minor modifications.[23] Collected 50 mL of untreated sewage from the Second Affiliated Hospital of Anhui Medical University and removed impurities and bacteria from the sewage by centrifugation and a 0.22 μm filter (Sangon Biotech Co., Shanghai, China). KP1049 (K1 *K. pneumoniae*) was selected as the host bacterium, single colony was picked with a sterile inoculation loop, inoculated into LB medium, and incubated into the logarithmic growth phase at 37 °C and 160 rpm. The filtrate was added to the KP1049 bacterial suspension and incubated overnight. The mixture was filtered and the phage was purified using a double-layer plaque assay. The filtrate was diluted with SM buffer and 10 μL of the diluted filtrate was added to 400 μL of the KP1049 bacterial suspension. The solution was incubated at 37 °C for 15 min, after which 3 mL of LB medium containing 0.7% agar was added, mixed well, and poured onto LB agar plates. The plates were incubated overnight at 37 °C. Single plaques from these plates were picked and cultured in LB medium supplemented with the host bacteria over night at 37 °C and 160 rpm. The culture was filtered to remove bacteria and subjected to a double-layer plaque assay to isolate the phage. This process was repeated until uniform plaques appeared on the plate, indicating that the filtrate was a purified phage suspension, and the phage was named vB_Kpn_HF0522.

## Genomic Sequence Analysis

In order to gain a deeper understanding of the genetic information and evolutionary relationships of the phage, we extracted the genes of the phage and performed gene sequencing analysis. Phages were concentrated using a previously described polyethylene glycol (PEG) precipitation method.[37] Phage DNA was extracted using a Viral RNA/DNA Extraction Kit (Takara, Japan) according to the manufacturer's instructions. The phage genome was sequenced using the Illumina NovaSeq platform and assembled with A5-MiSeq v20160825 (https://arxiv.org/abs/1401.5130) and SPAdes v3.12.0 (http://cab.spbu.ru/files/release3.12.0/manual.html).[38,39] Open reading frame (ORF) prediction was performed using a database (https://www.ncbi.nlm.nih.gov/orffinder/), while tRNAscan-SE2 (http://lowelab.ucsc.edu/cgi-bin/tRNAscan-SE2.cgi) was used to detect the presence of tRNA.[40] Virulence and resistance genes were identified using VirulenceFinder (https://cge.cbs.dtu.dk/services/VirulenceFinder/) and ResFinder (https://cge.cbs.dtu.dk/services/ResFinder/).[41] The phylogenetic tree was constructed using the amino acid sequences of the DNA polymerase and major head proteins, applying the neighbor-joining method with 1000 bootstrap replications in MEGA 11.[42] BLAST analysis and BLAST Ring Image Generator were used to compare the sequences of the genomes.[43]

## Transmission Electron Microscopy

The phage morphology was analyzed using transmission electron microscopy (TEM). The purified vB_Kpn_HF0522 (20 μL) was placed on a carbon-coated copper grid and left to stand for 5 min. Next, 2% (w/v) phosphotungstic acid (PTA) was used to stain the sample negatively and was observed under a transmission electron microscope (Hitachi HT7800, Japan).

## Host Range

The host range of vB_Kpn_HF0522 was confirmed by the double-layer plaque assay, which was used to determine whether the lysis of the phage was specific. The 47 nonrepetitive *K. pneumoniae* strains used in this study were collected from routine clinical samples at the hospital. All strains were preserved in LB medium supplemented with 20% glycerol and stored at −80°C for long-term storage. The bacterial suspension in the logarithmic growth phase was spread evenly on LB agar plates, 5 μL of phage suspension was dropped onto the plates, and the plates were incubated at 37 °C overnight. The host range of vB_Kpn_HF0522 was preliminarily determined based on the presence or absence of plaques.[44] To further review the lysing ability of the phage, we examined the efficiency of plating (EOP) of the phage using the double-layer plaque assay for strains that can interact with phage and form plaques. The EOP was calculated as the ratio of plaques formed on target bacteria to those formed on host bacteria (KP1049).[45]

## Multiplicity of Infection (MOI) and One-Step Growth Curve of vB_Kpn_HF0522

The bacterial suspension ($1\times10^8$ CFU/mL) was prepared, and equal volumes of the diluted phage suspension were added at different MOIs, mixed well, and incubated at 37 °C for 15 min. 10 mL of LB medium was added to the mixture, followed by incubation at 37 °C and 160 rpm for 6 h. The suspensions were obtained by filtration and the phage titer was determined. The optimal MOI was determined by choosing the group with the highest phage titer, and the experiment was repeated thrice.[44]

Equal volumes of vB_Kpn_HF0522 and KP1049 bacterial suspensions were mixed at the optimal MOI, incubated at 37 °C for 15 min to allow binding, and centrifuged at 10,000 rpm for 5 min, and wash off the unbound phage with phosphate buffer solution (PBS). The pellet was resuspended in 20 mL of LB medium and cultured at 37 °C and 160 rpm for 80 min.[25] Samples were taken every 5 min, and the phage titer was determined by the double-layer plaque assay. The experiment was repeated thrice, and the average value was used to plot the one-step growth curve.

## Temperature and UV Stability

1mL of phage was placed in a water bath at different temperatures, incubated for 60 min, and then quickly placed on ice to cool down after the water bath. The phage titer was detected by the double-layer plaque assay, and the stability of the phage to temperature was analyzed.

To test the sensitivity of the phage to ultraviolet light, 10 mL of phage suspension was added to a sterile Petri dish and exposed to continuous UV irradiation (254 nm) for 2 h. Samples were collected every 20 min to measure the phage titer.[44] Three replicates were performed for each experiment.

## Adsorption Assay

A mixture of phage and KP1049 bacterial suspensions was incubated at 37 °C for 15 min at the optimal MOI. The samples were collected every 5 min and centrifuged at 10,000 rpm for 5 min. The supernatant was serially diluted with SM buffer to measure the titer of the unadsorbed phage. The adsorption ability of the phage was assessed over 15 min, with each experiment performed in triplicates.[23]

## Antibacterial Activity of vB_Kpn_HF0522 Against KP1049 in vitro

To initially assess the antibacterial activity of vB_Kpn_HF0522, we examined the growth curves of the bacteria in vitro. The phage and KP1049 suspensions were mixed at different MOIs (MOI = 10, MOI = 1, MOI = 0.1, MOI = 0.01, MOI = 0.001, MOI = 0.0001) and incubated at 37 °C and 160 rpm for 12 h. Analyses of the phage's inhibitory effect on bacterial growth were analyzed by collecting samples every 1 h and measuring the absorbance at 600 nm.[23]

## Evaluation of the Ability of Phage to Disrupt and Inhibit Biofilms

To determine whether the phage was capable of disrupting preformed biofilms, 200 μL of KP1049 suspension ($1\times10^6$ CFU/mL) was added to a 96-well plate and incubated at 37 °C for 48 h. The bacterial suspension was carefully discarded, and the planktonic bacteria were washed away with PBS. 200 μL different titers of phage suspensions (MOI = 10, MOI = 1, MOI = 0.1, MOI = 0.01, MOI = 0.001, and MOI = 0.0001) were added to the

wells, and LB medium was added to the control group. After 12 h of incubation, the wells were washed thrice with PBS and stained with crystal violet. The staining solution was rinsed with PBS at the end of the staining process and 200 μL of ethanol was added to dissolve the stain. A microplate reader was used to measure absorbance at 570 nm to evaluate the effects of different phage titers on biofilm disruption.[23]

To inhibit biofilm formation, 100 μL of KP1049 ($1\times10^6$ CFU/mL) and different titers of phage suspensions (MOI = 10, MOI = 1, MOI = 0.1, MOI = 0.01, MOI = 0.001, and MOI = 0.0001) were added to a 96-well plate. The plate was incubated at 37 °C for 48 h, and biofilm formation was assessed by the crystal violet staining assay.[46] The results of the phage and control groups were compared to determine whether the phage inhibited biofilm formation.

## Growth Curve and Pathogenicity Determination of Phage-Resistant Mutant Bacteria

To clarify the effect of phage resistance mutations on the therapeutic efficacy of phage, we isolated phage-resistant mutant bacteria in vitro and monitored the growth curve and virulence of the bacteria. The host bacteria and phage were co-cultured at 37 °C for a period of time, and the bacterial suspension was collected after the liquid changed from clear to turbid. The strains were inoculated onto LB agar plates using a sterile inoculation loop and placed at 37 °C for overnight incubation. The isolated mutant strain was named as P-mut-KP1049.

KP1049 and P-mut-KP1049 were cultured in LB medium until logarithmic growth stage, respectively, and 400 μL of bacterial suspension ($1\times10^8$ CFU/mL) was taken and added to 40 mL of LB medium, mixed well, and then incubated at 160 rpm at 37 °C for 12 h. During this period, the suspension was taken out to detect its absorbance at 600 nm every hour and the bacterial growth curve was plotted based on the average of the results of three replicated experiments.

To validate the pathogenicity of P-mut-KP1049 in a mouse infection model, 6–8-week-old female BALB/c mice were selected for the study. The mice were randomly divided into five groups of eight mice each. Mice in group A were injected intraperitoneally with 100 μL of PBS. Mice in groups B and C were injected with different doses of KP1049 bacterial suspension, in which group B was injected with $1\times10^7$ CFU and group C was injected with $1\times10^6$ CFU; mice in groups D and E were injected with different doses of P-mut-KP1049 bacterial suspension, in which group D was injected with $1\times10^7$ CFU and group E was injected with $1\times10^6$ CFU. The experiment was repeated three times, the survival rate of mice was recorded continuously for 7 days, and the pathogenicity of the mutant strain was analyzed based on the survival rate of mice.

## Therapeutic Potential of vB_Kpn_HF0522 in the G. mellonella Infection Model

To analyze the ability of vB_Kpn_HF0522 to eliminate pathogens in vivo, a *G. mellonella* infection model was constructed. *G. mellonella* approximately 25 mm in length and vigorous, was selected for this study. To determine the optimal bacterial infection dose, *G. mellonella* was randomly divided into eight groups, including a PBS group and groups with different concentrations of bacteria ($1\times10^4$, $1\times10^5$, $1\times10^6$, $1\times10^7$, $3\times10^7$, $6\times10^7$, and $1\times10^8$ CFU/mL). Based on survival after injection, a concentration of $3\times10^7$ CFU/mL was selected as the final experimental dose.

Each group contained eight larvae, which were subsequently placed in sterile petri dishes. The groups included experimental group, blank group, and phage treatment groups at different doses. In the blank group, *G. mellonella* was injected with 10 μL of PBS on the right second hindfoot. In the experimental group and phage treatment groups, *G. mellonella* was injected with 10 μL of KP1049 bacterial suspension ($3\times10^7$ CFU/mL) in the logarithmic growth phase. The *G. mellonella* were placed in a humidified chamber at 37 °C in the dark for 1 h. After 1 h, the phage treatment groups were injected with phage suspensions at different MOIs (MOI = 10, MOI = 1, MOI = 0.1, MOI = 0.01, MOI = 0.001, and MOI = 0.0001), while the other groups received 10 μL of sterile PBS. Three replicate experiments were conducted to determine the average survival of *G. mellonella* over a five-day period and the results were used to plot the survival curve.

## Efficacy of vB_Kpn_HF0522 in an Incisional Surgical Site Infection Model

An incisional surgical site infection model was constructed to simulate human wound healing, and the therapeutic effect of the phage on surgical wound infections was analyzed.[47] 6–8-week-old female BALB/c mice were selected for this test and the mice were divided into groups of 8 each. The mice were anesthetized via intraperitoneal injection of tribromoethanol

(0.2 mL/10 g body weight in a 1.2% solution). After the dorsal hair was shaved and disinfected with 75% ethanol, a 1 cm incision extending to the deep fascia was created on one side of the spine using a sterile scalpel. A surgical thread was used to suture the wound. KP1049 suspension (50 μL, $1\times10^5$ CFU/mL) was inoculated into the suture site. After 1 h, 50 μL of vB_Kpn_HF0522 suspension ($1\times10^7$ PFU/mL) was injected subcutaneously at the surgical wound site, whereas the blank group was injected with an equal volume of PBS. The efficacy of phage treatment was evaluated by monitoring the wound recovery over time. The experiment was repeated three times to ensure the accuracy of the results.

## Statistical Analysis

The data were statistically analyzed using GraphPad Prism 9.5.0 and SPSS 27.0, and are presented as mean values and standard deviations. Comparisons of differences in means between groups affected by a single variable were analyzed by one-way ANOVA, and $P < 0.05$ was considered to indicate statistical significance. The Cox proportional hazards model was used to analyze the effects of the variables on the survival rates of *G. mellonella* and mice.

# Results

## Phage Isolation and Morphological Analysis

KP1049 was used as the host bacterium to isolate phage vB_Kpn_HF0522 from the hospital sewage. Clear plaques with halos were observed on the KP1049 lawn (Figure 1A). TEM revealed that the phage had an icosahedral head with a diameter of 59.33±2.04 nm and a tail with a diameter of 20.02±1.56 nm (Figure 1B).

## Genomic Analysis

Genomic analysis revealed that vB_Kpn_HF0522 possessed a linear double-stranded DNA sequence of 42,437 bp, with a GC content of 54.17%. The sequences were uploaded to the NCBI database (GenBank accession number PP836776.1). Bioinformatics analysis revealed 50 open reading frames (ORFs), 24 of which encoded functional proteins, whereas the rest were hypothetical proteins. Further analysis revealed that no virulence or antibiotic resistance genes were present, indicating that this phage can be used in various ways. The phage genome does not contain tRNA genes. BLASTn analysis revealed that vB_Kpn_HF0522 was similar to *Klebsiella* phage P284 (PP934444.1), *Klebsiella* phage Henu1_1 (PQ133006.1), *Klebsiella* phage Phi_K2044 (PP442062.1), *Klebsiella* phage pKP-M212-2.1 (OQ734493.1), *Klebsiella* phage Henu1_2 (PQ133005.1), *Klebsiella* phage xx20 (OQ871562.1), *Klebsiella* phage RCIP0049 (OR532843.1), and *Klebsiella* phage vB_Kp_XP4 (PP663283.1), with >95% identity; these phages belong to the genus Drulisvirus (Figure 2), and the host bacteria of these phages are all *K. pneumoniae*.

Evolutionary analysis of conserved DNA polymerase genes (Figure 3A) and major head proteins (Figure 3B) suggested that vB_Kpn_HF0522 is closely related to *Klebsiella* phage P284 (GenBank: PP934444.1) and *Klebsiella* phage KP_NC6 (GenBank: PQ530295.1), which belong to the genus Drulisvirus. Based on the genomic information and the results of TEM analysis, vB_Kpn_HF0522 should be classified under the genus Drulisvirus.

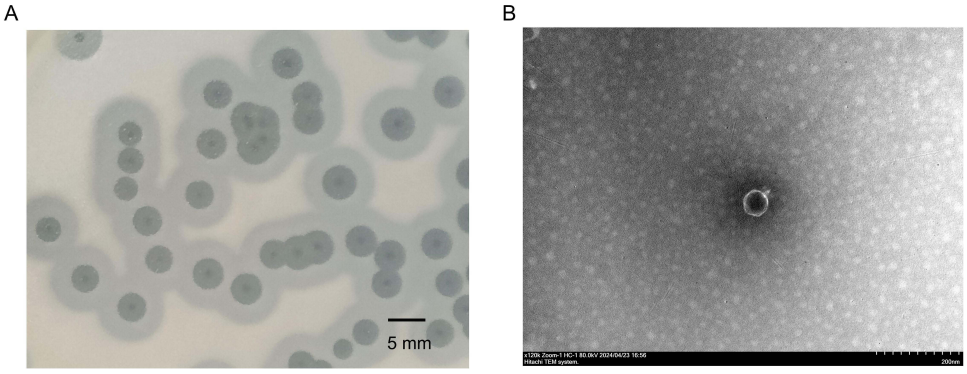


**Figure 1** Characteristics of phage vB_Kpn_HF0522. (**A**) Plaques formed by phage vB_Kpn_HF0522. (**B**) Morphology of phage vB_Kpn_HF0522 under TEM. The scale bars represent 200 nm.

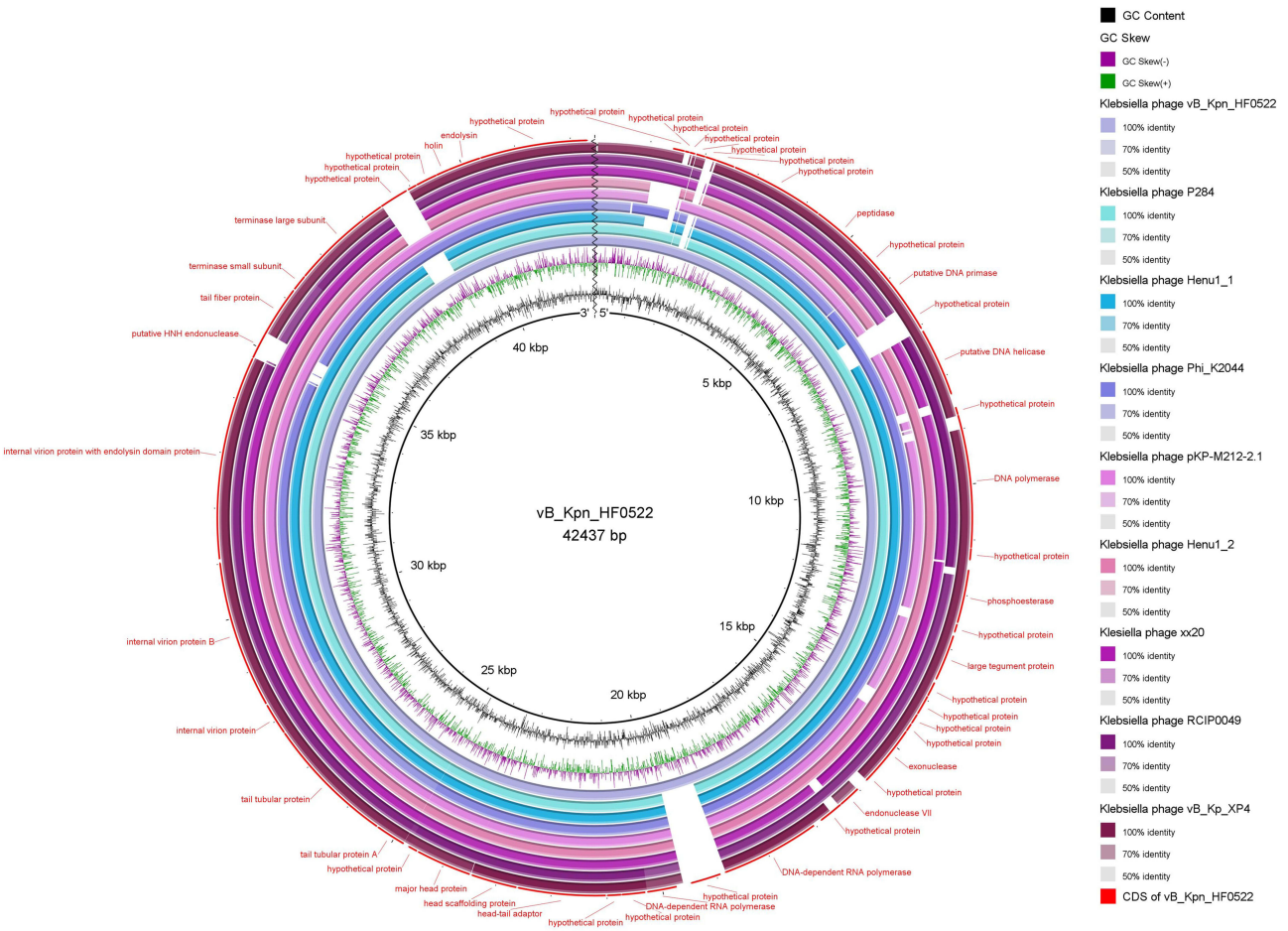


**Figure 2** Characteristics of the complete genome of phage vB_Kpn_HF0522. Comparative genomic analysis of vB_Kpn_HF0522 with other highly similar phages. Taking the complete sequence of vB_Kpn_HF0522 as a reference, the white and colored regions in the circles indicate absence and presence. The circles from inside to outside indicate the GC content of vB_Kpn_HF0522, the GC skew of vB_Kpn_HF0522, vB_Kpn_HF0522 (PP836776.1), *Klebsiella* phage P284 (PP934444.1), *Klebsiella* phage Henu1_1 (PQ133006.1), *Klebsiella* phage Phi_K2044 (PP442062.1), *Klebsiella* phage pKP-M212-2.1 (OQ734493.1), *Klebsiella* phage Henu1_2 (PQ133005.1), *Klebsiella* phage xx20 (OQ871562.1), *Klebsiella* phage RCIP0049 (OR532843.1), *Klebsiella* phage vB_Kp_XP4 (PP663283.1) and the CDS of vB_Kpn_HF0522.

## Physiological Characterization of Phage vB_Kpn_HF0522

vB_Kpn_HF0522 was mixed and cultured with KP1049 at different MOIs, and phage titer was detected after 6 h. The phage titer in the group with an MOI = 0.01 was significantly greater than that in the other groups, indicating that an MOI of 0.01 was the optimal MOI for vB_Kpn_HF0522 (Figure 4A). vB_Kpn_HF0522 and KP1049 were mixed in LB medium, and a one-step growth curve was generated according to the change in the phage titer. The vB_Kpn_HF0522 titer increased more slowly at 0–15 min and then increased rapidly after 15 min until it reached a plateau at approximately 60 min, indicating that its latency period was approximately 15 min, and its lysis period was approximately 45 min (Figure 4B). By testing the adsorption capacity of vB_Kpn_HF0522, it was found that more than 90% of the phage was adsorbed onto the host bacteria after 15 min of co-culture with the bacteria (Figure 4C). The presence of active phages was still detected after incubation of phage at below 60 °C for 1h, but all phages died after incubation at 70 °C (Figure 4D). UV stability tests revealed that phage titers decreased with increasing UV irradiation time (Figure 4E).

## Host Range

The 47 strains used in this study included types K1, K2, K16, K19, K20, K24, K28, K30, K38, K41, K47, K51, K62, K63, and K64. The results showed that the phage formed clear plaques on plates inoculated with K1 *K. pneumoniae* bacterial suspension, surrounded by a translucent halo. This phage had lytic activity against nine strains of K1 *K. pneumoniae* but no lytic activity against the remaining *K. pneumoniae* strains. Thus, it can be inferred that the


https://doi.org/10.2147/IDR.S501921

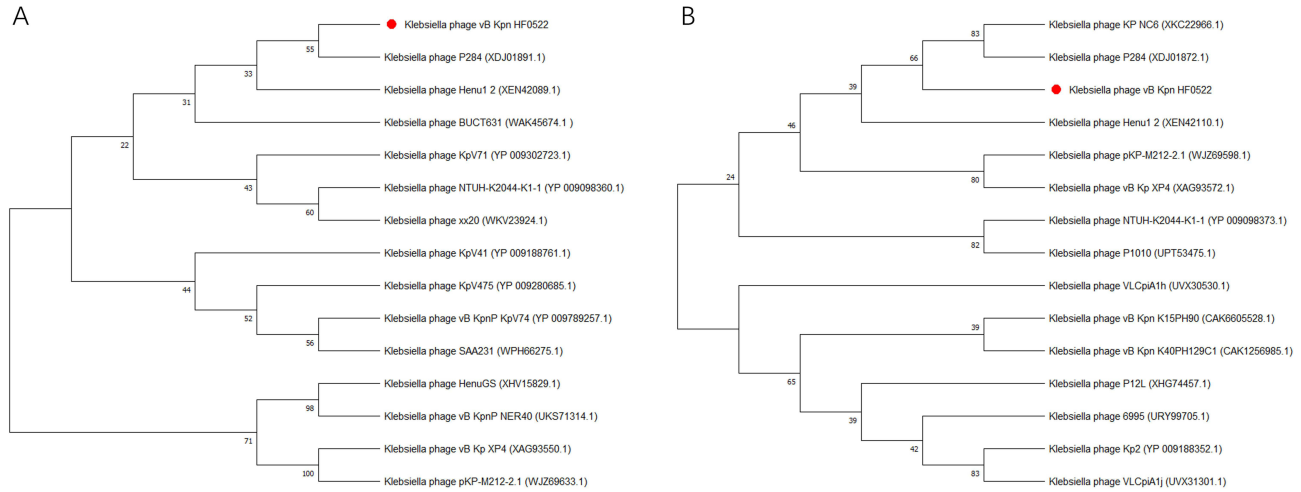


**Figure 3** Phylogenetic analyses of vB_Kpn_HF0522. The phylogenetic trees of phage vB_Kpn_HF0522 were constructed in MEGA 11 via the neighbor-joining method with 1000 bootstrap repeats based on the amino acid sequence composition of its DNA polymerase (**A**) and major head protein (**B**). The amino acid sequences of the relevant phages were downloaded from NCBI.

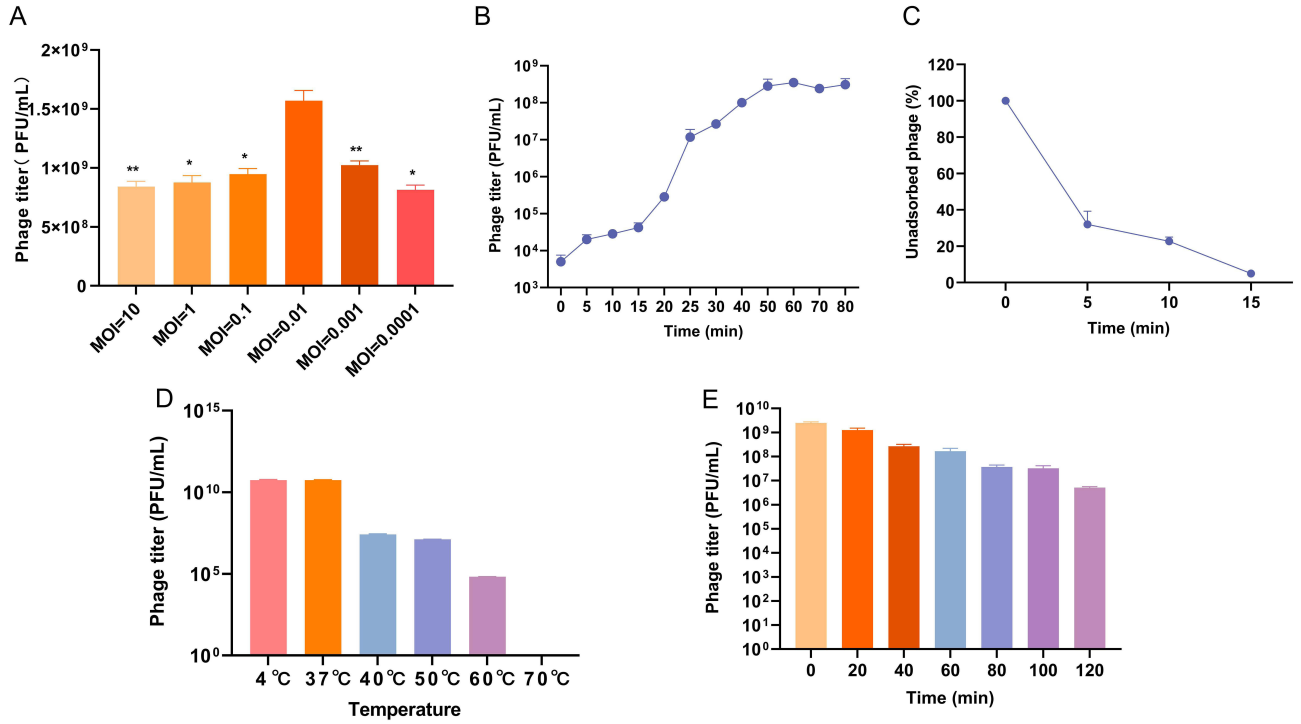


**Figure 4** Biological characteristics of phage vB_Kpn_HF0522. (**A**) Optimal MOI assays of vB_Kpn_HF0522 (*$P < 0.05$, ** $P < 0.01$ indicate a significant difference compared with MOI = 0.01). (**B**) One-step growth curve of vB_Kpn_HF0522. (**C**) Adsorption curve of vB_Kpn_HF0522. (**D**) Temperature stability of vB_Kpn_HF0522. (**E**) Ultraviolet stability of vB_Kpn_HF0522.

phage specifically lyses K1 *K. pneumoniae* (Table 1). This property makes phages promising for application in the characterization of the bacterial capsular type.

## Antibacterial Activity of Phage Against KP1049 in vitro

KP1049 and vB_Kpn_HF0522 were co-cultured at different MOIs for 12 hours. The OD600 values were measured to monitor bacterial growth, and growth curves were plotted based on the results. During the first 11 h of co-culture, the absorbance of bacteria in the phage-treated group remained consistently lower than that of KP1049. However, starting

**Table 1** Host Range of vB_Kpn_HF0522

| *K. pneumoniae* strains | Capsular type | Plaques | Halos | EOP |
|---|---|---|---|---|
| KP42545 | K1 | + | + | 0.70 |
| KP41164 | K1 | + | + | 0.91 |
| KP46108 | K1 | + | + | 0.75 |
| KP51186 | K1 | + | + | 0.38 |
| KP47198 | K1 | + | + | 0.06 |
| KP47783 | K1 | + | + | 0.64 |
| KP27359 | K1 | + | + | 0.77 |
| KP04943 | K1 | + | + | 0.82 |
| KP1049 | K1 | + | + | 1 |
| KP25915, KP26666, KP26328 | K2 | – | – | – |
| KP10429 | K16 | – | – | – |
| KP15380, KP86078, KP19057 | K19 | – | – | – |
| KP41665, KP29379, KP26154 | K20 | – | – | – |
| KP21756, KP22274, KP23347 | K24 | – | – | – |
| KP51072, KP81054, KP91019 | K28 | – | – | – |
| KP71062, KP62643, KP61130 | K30 | – | – | – |
| KP08696 | K38 | – | – | – |
| KP25632, KP19701, KP28371 | K41 | – | – | – |
| KP10471, KP15752, KP71017 | K47 | – | – | – |
| KP27098, KP30188, KP03507 | K51 | – | – | – |
| KP43200, KP41034, KP22849 | K62 | – | – | – |
| KP71019, KP14966, KP01070 | K63 | – | – | – |
| KP71023, KP01063, KP10533 | K64 | – | – | – |

**Notes**: - no lysis; + showed plaques or halos. Phage efficiency was classified as high (EOP ≥ 0.5), medium (0.1 ≤ EOP < 0.5), low (0.001 < EOP <0.1), or inefficient (EOP ≤ 0.001).

from the 9th hour, the absorbance of the phage-treated group gradually increased, reaching levels comparable to those of KP1049 by the 12th hour. This likely resulted from bacterial mutations induced by phage pressure, which allowed the bacteria to resist phage invasion (Figure 6A).

## Evaluation of the Ability of Phage to Disrupt and Inhibit Biofilms

To determine whether vB_Kpn_HF0522 could disrupt biofilms, KP1049 was cultured for 48 h to form biofilms, followed by the addition of various concentrations of vB_Kpn_HF0522 and further incubation for 12 h. Crystal violet staining indicated that vB_Kpn_HF0522 disrupted biofilms at various MOIs (Figure 5A). Furthermore, phage inhibited biofilm formation when mixed with KP1049 at different MOIs (Figure 5B). However, the groups did not exhibit a clear dose-dependent response to the phages, and it was may be due to the bacterial mutations induced by phages.


https://doi.org/10.2147/IDR.S501921

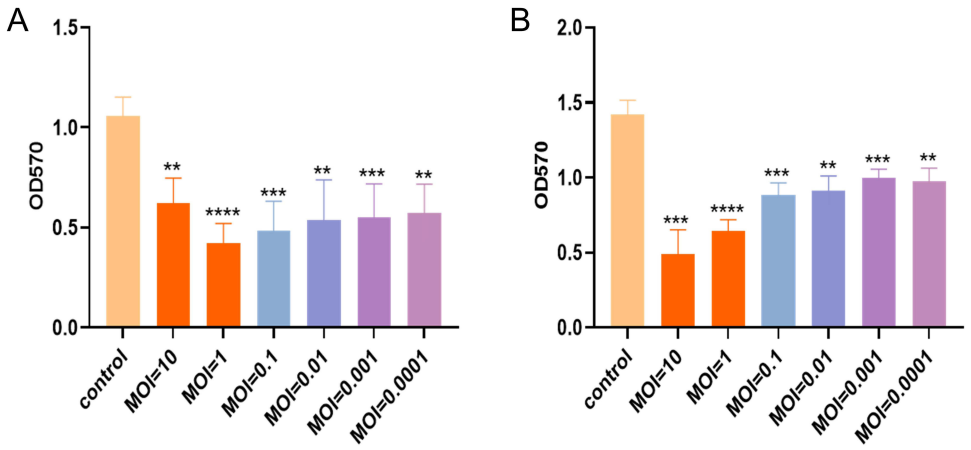


**Figure 5** Evaluation of phage disruption and inhibition of biofilms. (**A**) The biofilm disruption effect of phage vB_Kpn_HF0522. (**B**) The biofilm inhibition effect of phage vB_Kpn_HF0522. (**$P < 0.01$, *** $P < 0.001$ and **** $P < 0.0001$ indicate significant differences compared with the control group).

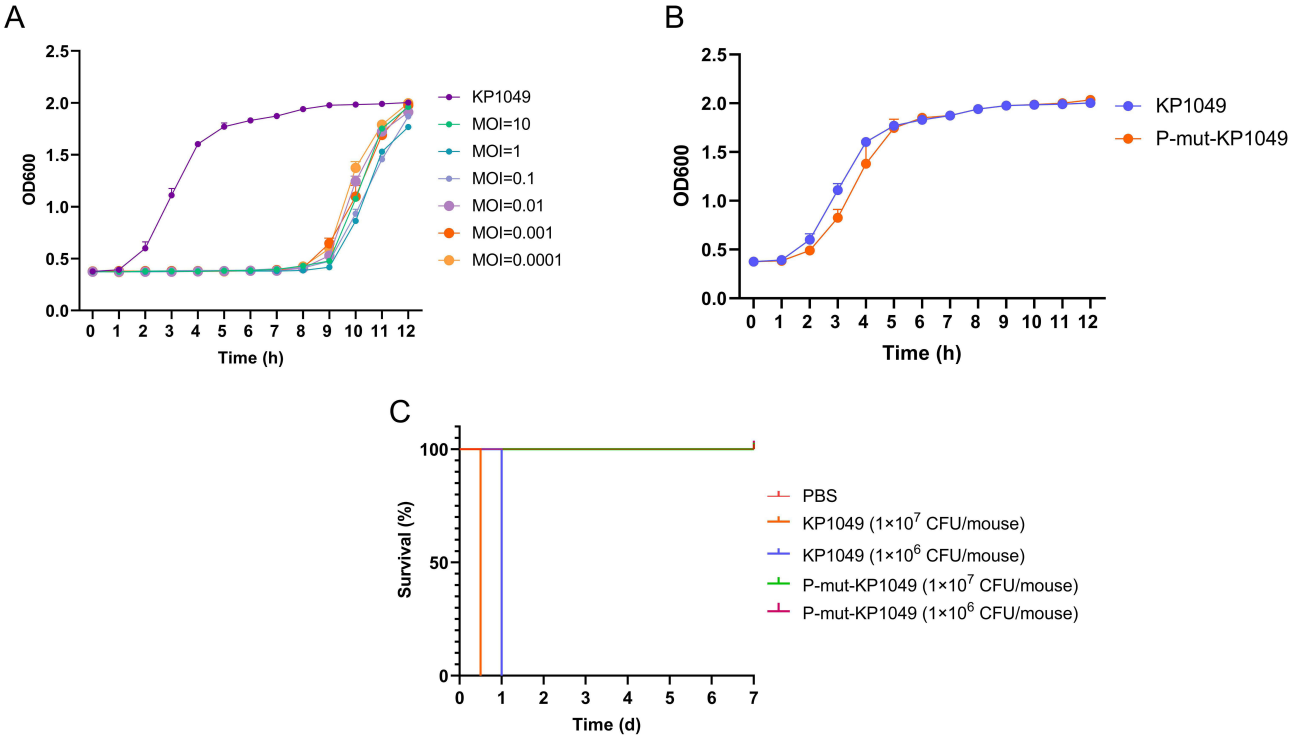


**Figure 6** Bacterial growth curves and pathogenicity of KP1049 and phage-resistant mutant bacteria (**A**) Bacterial growth curves under various MOIs. (**B**) Growth curves of KP1049 and phage mutant bacteria. (**C**) Survival of mice infected with different doses of KP1049 or P-mut-KP1049.

## Growth Curve and Pathogenicity Determination of Phage-Resistant Mutant Bacteria

After co-culturing the phage with bacteria, the medium transitioned from clear to turbid and the bacteria were collected for further experiments. Comparing the growth curves of KP1049 and P-mut-KP1049, it was observed that P-mut-KP1049 grew slower than KP1049 during the first 4 h, but growth rates converged thereafter (Figure 6B).

In the mouse infection model, the survival rate of mice infected with the mutant strain was significantly higher than that of mice those infected with KP1049, suggesting that the phage-resistant mutants may not compromise the therapeutic efficacy of the phage (Figure 6C).

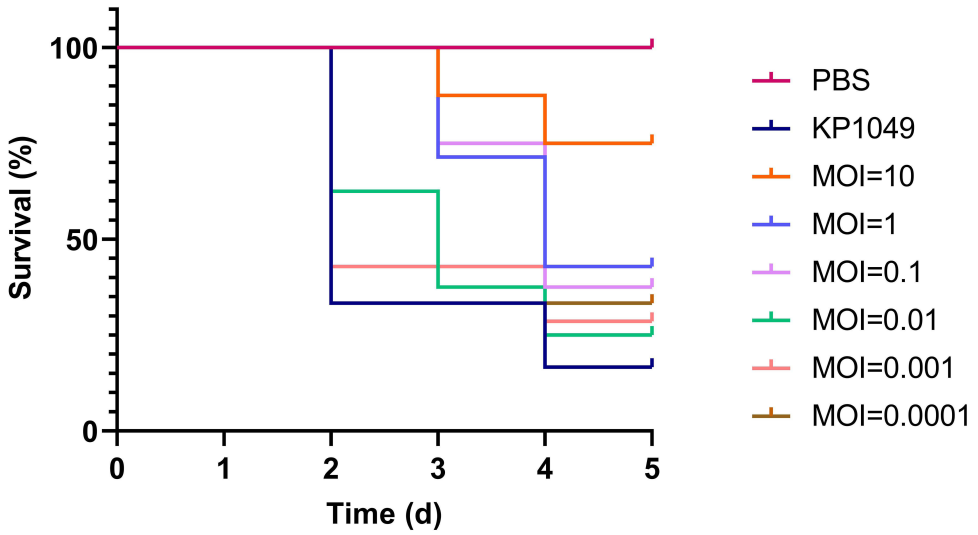


**Figure 7** Survival rate of *G. mellonella* in different groups. The five-day survival rate was 12.5% in the experimental group (group = KP1049) and 100% in the blank group (group = PBS). *G. mellonella* survival varied with different doses of phage, with a maximum of 75% (group = MOI = 10).

## Antibacterial Activity of vB_Kpn_HF0522 in the G. mellonella Infection Model

To test the effect of the phage in vivo, we constructed a *G. mellonella* infection model and treated infected *G. mellonella* with different doses of the phage to observe its effect on the survival rate of *G. mellonella*. The survival rate of the experimental group decreased to 50% after 24 h of infection and to 12.5% after 4 days, whereas the phage-treated group (MOI = 10) achieved a five-day survival rate of 75% (Figure 7). This result demonstrates that vB_Kpn_HF0522 has the potential to fight infection in vivo.

## Evaluation of Phage Therapeutic Potential in an Incisional Surgical Site Infection Model

An incisional surgical site infection model was established to simulate human wound recovery and to evaluate the therapeutic potential of vB_Kpn_HF0522 for surgical wound infections. Three days after infection, the wounds of untreated mice showed significant edema, pus accumulation, and deformity of the underlying fascia. In contrast, the phage treatment group presented no obvious redness or swelling, scab formation at the incision site, and clear subcutaneous tissues without adhesion or purulent exudate formation. The results of HE analysis indicated significant infiltration of inflammatory cells and disorganized fiber arrangement in the skin tissue of mice in the experimental group, suggesting strong inflammatory activity. In contrast, the skin tissue of mice in the phage treatment group showed less inflammatory cell infiltration, with an overall more intact structure and relatively mild inflammatory response. On the seventh day post-infection, a large accumulation of pus was still observed in the subcutaneous tissue of mice in the experimental group, whereas the skin tissue of mice in the phage treatment group and the control group showed good healing (Figure 8). This demonstrates that phage vB_Kpn_HF0522 has the potential to control surgical site infections.

# Discussion

K1 *K. pneumoniae* is a highly pathogenic strain known to cause invasive community-acquired infections, such as liver abscesses, meningitis, and sepsis.[5] This strain is particularly prevalent in Asia but has increased worldwide in recent years.[48,49] Phage therapy is considered a supplementary or alternative treatment to antibacterial agents, and numerous clinical cases in recent years have suggested that phages possess antibacterial capabilities in vivo. Previous studies have analyzed the therapeutic potential of the K1 *K. pneumoniae* phage,[23–25,50] but the effect of phage resistance mutation on disease treatment is still unclear, and surgical infection models that validate the effects of phages have not been adequately defined. The development of new phages can provide broader clinical application options, and studying their potential offers theoretical support for phage therapies.


https://doi.org/10.2147/IDR.S501921

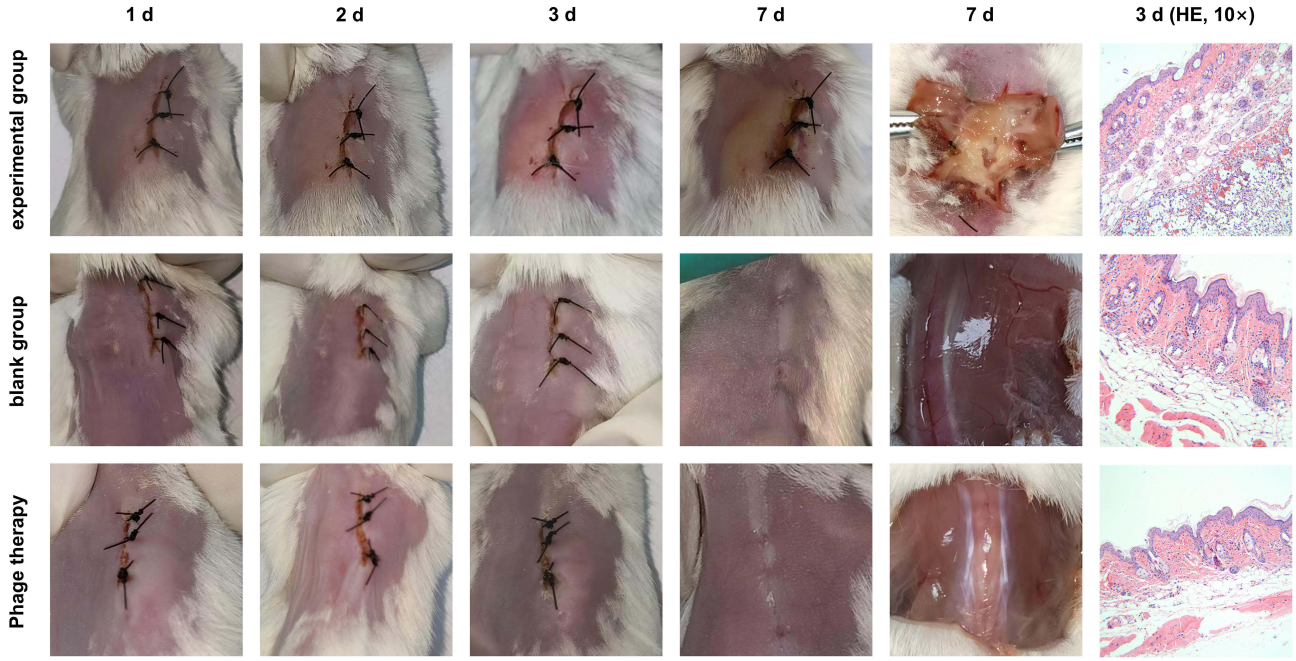


**Figure 8** The incisional healing conditions of the three groups of mice. HE-stained images were taken at a magnification of 10×.

In this study, we isolated a phage strain from sewage named vB_Kpn_HF0522. TEM revealed that the phage had an icosahedral head with a diameter of 59.33±2.04 nm and a tail with a diameter of 20.02±1.56 nm. Genomic analysis showed that vB_Kpn_HF0522 is a double-stranded linear DNA virus that lacks virulence and antibiotic resistance genes, demonstrating that it is safe for in vivo therapeutic use. Bioinformatics analysis revealed 50 open reading frames (ORFs), 24 of which encoded functional proteins, whereas the rest were hypothetical proteins. Based on the genomic information and the results of TEM analysis, vB_Kpn_HF0522 should be classified under the genus Drulisvirus. Host range detection revealed that vB_Kpn_HF0522 specifically lysed the serotype K1 *K. pneumoniae*. Using this property, phage-targeted therapy as well as *K. pneumoniae* capsular serotypes identification can be carried out. Based on one-step growth and adsorption curve analysis, the phage had a latent period of approximately 15 min and a lytic period of approximately 45 min. Additionally, approximately 90% of the phages were able to adsorb onto host bacteria within the first 15 min. These results show that vB_Kpn_HF0522 is able to attach to host bacteria in a relatively short period of time, resulting in a rapid bactericidal effect.

The bacterial growth curves showed limited proliferation within the first 9 h of phage treatment. However, after 9 h, the bacterial numbers increased and approached those of KP1049 by the 12th hour, indicating the emergence of phage-resistant mutants during co-culture. During phage therapy, the emergence of phage-resistant mutant bacteria may occur, and such mutations are often accompanied by a fitness cost to the bacteria. Studies have shown that these mutations frequently result in a reduction in the bacteria's virulence.[51] To assess the effect of phage resistance mutations on therapy, we isolated a resistant mutant strain. First, to assess whether the mutation affects bacterial growth rate, we monitored the growth curves of the bacteria. The experimental results showed that within the first 4 hours, the growth rate of the phage-resistant mutant strain was slower than that of KP1049, but it gradually approached the growth level of KP1049 over time. These findings suggest that the phage resistance mutation has a minimal impact on bacterial growth rate. To further evaluate the impact of the phage mutation on therapeutic efficacy, we constructed a mouse infection model to investigate whether the virulence of the phage-resistant mutant strain had changed. In mouse infection models, the 7-day survival rate of P-mut-KP1049 infected mice was 100%, while KP1049 infected mice survived for less than 24 h. This result demonstrated that the mutation reduced the pathogenicity of the bacteria. Other similar studies have found that phage resistance mutations can result in bacteria that are less virulent and more adaptable This biological trade-off may impact the antibiotic resistance of these bacteria, leading to the loss of virulence factors and thereby making them more susceptible to recognition and clearance by the host immune system.[52] Therefore, we hypothesize that mutation does

not significantly affect phage therapeutic efficacy. Biofilm formation is one of the key pathogenic mechanisms of *K. pneumoniae*, as it shields bacteria from antibiotics and the host immune system, leading to chronic and persistent infections.[53,54] Therefore, we aimed to experimentally assess the ability of the phage to disrupt and inhibit biofilm formation. Although phages vB_Kpn_HF0522 effectively disrupted and inhibited biofilms, they did not completely eliminate biofilms, likely because of the development of phage-resistant bacterial mutants. One study also showed that phage-free tail fiber proteins can interact with bacterial capsules within biofilms, leading to capsule degradation. Because the capsule serves as a receptor for phage binding to bacteria, the absence of the capsule prevents the phage from effectively binding to and killing bacteria.[55]

To preliminarily evaluate the potential application of phages in treating infections in vivo, we established a *G. mellonella* infection model and treated it with phages at varying titers. The results showed that vB_Kpn_HF0522 significantly increased the survival rate of infected *G. mellonella*, with the survival rate increasing from 12.5% to 75% at an MOI of 10, indicating that vB_Kpn_HF0522 could exert anti-infective effects in vivo. *K. pneumoniae* can cause SSI, posing a significant challenge to clinical care.[56,57] In this study, we developed an incisional surgical site infection model to evaluate the therapeutic potential of phages in such infections, aiming to provide new insights and approaches for clinical treatment. In an incisional surgical site infection model, the group treated with phage showed significantly better outcomes than experimental group, displaying a normal healing cycle and less abscess formation, highlighting the potential of vB_Kpn_HF0522 in controlling incisional surgical site infections. In clinical practice, skin and soft tissue abscesses are typically treated with intravenous antimicrobial agents, necessitating multiple doses throughout the treatment cycle to maintain effective drug concentrations in the body.[58,59] In this study, the phage was directly delivered in situ via subcutaneous injection, thereby reducing the necessity for invasive procedures throughout the entire treatment period. It is therefore concluded that phage vB_Kpn_HF0522 has significant therapeutic potential for the control of infections caused by these bacteria, and is expected to be applied in personalized clinical therapy.

Although this study demonstrated the effectiveness of phage therapy in combating bacterial infections, we must acknowledge certain limitations. The experiments were conducted in simplified models that do not fully replicate the complexity of human infections. Future research should focus on evaluating the efficacy of phage therapy in more clinically relevant models and developing phage cocktail therapies to provide stronger scientific support for its clinical application.

## Conclusion

In this study, we successfully isolated and characterized phage vB_Kpn_HF0522, a promising candidate for combating K1 *K. pneumoniae* infections. The phage demonstrated robust lytic activity, the ability to disrupt biofilms, and therapeutic potential in both in vitro and in vivo models. Notably, the phage improved prognosis in incisional surgical site infections in mice, emphasizing its potential clinical applicability. Moreover, while phage-resistant mutants emerged during the experiments, these mutations were associated with reduced bacterial virulence, suggesting a biological trade-off that might mitigate their clinical impact. This study highlights the potential of phage vB_Kpn_HF0522 as a safe and effective therapeutic agent. Further exploration of phage therapy mechanisms and clinical verification are imperative for a comprehensive comprehension of its applicability and the resolution of potential challenges.

## Ethics Statement

All animals used in this study were reviewed and approved by the Institutional Animal Care and Use Committee of Anhui Medical University (approval number: LLSC20240703), and all experiments were performed in accordance with the guidelines. This study was approved by the ethics committee of the hospital (approval number: KYLL20240200).

## Funding

This work was supported by Anhui Provincial Natural Science Foundation (2408085MH233), Research Fund of Anhui Institute of Translational Medicine (2023zhyx-C78), the project of Anhui Province Key Laboratory of Infectious Diseases, The First Affiliated Hospital of Anhui Medical University (AHIDL-2412R), National Natural Science

Foundation of China (82302534), Anhui Province Scientific Research Compilation Plan Project (2022AH050730), and Natural Science Research Project of Anhui Educational Committee (2023AH053175).

## Disclosure

The authors declare that there are no conflicts of interest in this work.

## References


1. Zhang X, Yang Q, Gao B, et al. *Klebsiella pneumoniae* infection associated septic pulmonary embolism in an emergency department from East China. *Ann Palliat Med*. 2021;10(2):1521–1529. doi:10.21037/apm-19-648
2. Russo TA, Marr CM. Hypervirulent *Klebsiella pneumoniae*. *Clin Microbiol Rev*. 2019;32(3). doi:10.1128/CMR.00001-19
3. Singh AK, Mishra H, Firdaus Z, et al. MoS (2)-modified curcumin nanostructures: the novel theranostic hybrid having potent antibacterial and antibiofilm activities against multidrug-resistant hypervirulent *Klebsiella pneumoniae*. *Chem Res Toxicol*. 2019;32(8):1599–1618. doi:10.1021/acs.chemrestox.9b00135
4. Pei N, Liu Q, Cheng X, et al. Longitudinal study of the drug resistance in *Klebsiella pneumoniae* of a Tertiary Hospital, China: phenotypic epidemiology analysis (2013–2018). *Infect Drug Resist*. 2021;14:613–626. doi:10.2147/IDR.S294989
5. Sahoo M, Behera DU, Sahoo RK, et al. Synergistic action of 6-gingerol as an adjuvant to colistin for susceptibility enhancement in multidrug-resistant *Klebsiella pneumoniae* isolates. *RSC Adv*. 2024;14(11):7779–7785. doi:10.1039/D3RA07835C
6. Huang X, Li X, An H, et al. Capsule type defines the capability of *Klebsiella pneumoniae* in evading Kupffer cell capture in the liver. *PLoS Pathog*. 2022;18(8):e1010693. doi:10.1371/journal.ppat.1010693
7. Zhu J, Wang T, Chen L, et al. Virulence Factors in Hypervirulent *Klebsiella pneumoniae*. *Front Microbiol*. 2021;12:642484. doi:10.3389/fmicb.2021.642484
8. Qu TT, Zhou JC, Jiang Y, et al. Clinical and microbiological characteristics of *Klebsiella pneumoniae* liver abscess in East China. *BMC Infect Dis*. 2015;15:161. doi:10.1186/s12879-015-0899-7
9. Paczosa MK, Mecsas J. *Klebsiella pneumoniae*: going on the offense with a strong defense. *Microbiol Mol Biol Rev*. 2016;80(3):629–661. doi:10.1128/MMBR.00078-15
10. Wang L, Shen D, Wu H, et al. Resistance of hypervirulent *Klebsiella pneumoniae* to both intracellular and extracellular killing of neutrophils. *PLoS One*. 2017;12(3):e0173638. doi:10.1371/journal.pone.0173638
11. Shi Q, Lan P, Huang D, et al. Diversity of virulence level phenotype of hypervirulent *Klebsiella pneumoniae* from different sequence type lineage. *BMC Microbiol*. 2018;18(1):94. doi:10.1186/s12866-018-1236-2
12. Chen Y, Chen Y. Clinical challenges with hypervirulent *Klebsiella Pneumoniae* (hvKP) in China. *J Transl Int Med*. 2021;9(2):71–75. doi:10.2478/jtim-2021-0004
13. de la Fuente-Nunez C, Cesaro A, Hancock REW. Antibiotic failure: beyond antimicrobial resistance. *Drug Resist Updat*. 2023;71:101012. doi:10.1016/j.drup.2023.101012
14. La Rosa R, Johansen HK, Molin S. Persistent bacterial infections, antibiotic treatment failure, and microbial adaptive evolution. *Antibiotics*. 2022;11(3):419. doi:10.3390/antibiotics11030419
15. Bakkeren E, Diard M, Hardt WD. Evolutionary causes and consequences of bacterial antibiotic persistence. *Nat Rev Microbiol*. 2020;18(9):479–490. doi:10.1038/s41579-020-0378-z
16. Stojowska-Swędrzyńska K, Łupkowska A, Kuczyńska-Wiśnik D, et al. Antibiotic heteroresistance in *Klebsiella pneumoniae*. *Int J mol Sci*. 2021;23(1):449. doi:10.3390/ijms23010449
17. Kasman LM, Porter LD. Bacteriophages. In: *StatPearls*. Treasure Island (FL); StatPearls Publishing Copyright © 2024, StatPearls Publishing LLC; 2024.
18. Petrovic Fabijan A, Iredell J, Danis-Wlodarczyk K, et al. Translating phage therapy into the clinic: recent accomplishments but continuing challenges. *PLoS Biol*. 2023;21(5):e3002119. doi:10.1371/journal.pbio.3002119
19. Laforêt F, Antoine C, Lebrun S, et al. Impact assessment of vB_KpnP_K1-ULIP33 bacteriophage on the human gut microbiota using a dynamic in vitro model. *Viruses*. 2023;15(3):719. doi:10.3390/v15030719
20. Mu A, McDonald D, Jarmusch AK, et al. Assessment of the microbiome during bacteriophage therapy in combination with systemic antibiotics to treat a case of staphylococcal device infection. *Microbiome*. 2021;9(1):92. doi:10.1186/s40168-021-01026-9
21. Strathdee SA, Hatfull GF, Mutalik VK, et al. Phage therapy: from biological mechanisms to future directions. *Cell*. 2023;186(1):17–31. doi:10.1016/j.cell.2022.11.017
22. Hitchcock NM, Devequi Gomes Nunes D, Shiach J, et al. Current clinical landscape and global potential of bacteriophage therapy. *Viruses*. 2023;15(4):1020. doi:10.3390/v15041020
23. Han P, Pu M, Li Y, et al. Characterization of bacteriophage BUCT631 lytic for K1 *Klebsiella pneumoniae* and its therapeutic efficacy in *Galleria mellonella* larvae. *Virol Sin*. 2023;38(5):801–812. doi:10.1016/j.virs.2023.07.002
24. Zhao R, Jiang S, Ren S, et al. A novel phage putative depolymerase, Depo16, has specific activity against K1 capsular-type *Klebsiella pneumoniae*. *Appl Environ Microbiol*. 2024;90(4):e0119723. doi:10.1128/aem.01197-23
25. Pu M, Li Y, Han P, et al. Genomic characterization of a new phage BUCT541 against *Klebsiella pneumoniae* K1-ST23 and efficacy assessment in mouse and *Galleria mellonella* larvae. *Front Microbiol*. 2022;13:950737. doi:10.3389/fmicb.2022.950737
26. Tang M, Yao Z, Liu Y, et al. Host immunity involvement in the outcome of phage therapy against hypervirulent *Klebsiella pneumoniae* infections. *Antimicrob Agents Chemother*;2024. e0142923. doi:10.1128/aac.01429-23
27. Kuipers S, Ruth MM, Mientjes M, et al. A Dutch case report of successful treatment of chronic relapsing urinary tract infection with bacteriophages in a renal transplant patient. *Antimicrob Agents Chemother*. 2019;64(1). doi:10.1128/AAC.01281-19
28. Johri AV, Johri P, Hoyle N, et al. Case report: chronic bacterial prostatitis treated with phage therapy after multiple failed antibiotic treatments. *Front Pharmacol*. 2021;12:692614. doi:10.3389/fphar.2021.692614

29. Eskenazi A, Lood C, Wubbolts J, et al. Combination of pre-adapted bacteriophage therapy and antibiotics for treatment of fracture-related infection due to pandrug-resistant *Klebsiella pneumoniae*. *Nat Commun*. 2022;13(1):302. doi:10.1038/s41467-021-27656-z
30. Pires DP, Costa AR, Pinto G, et al. Current challenges and future opportunities of phage therapy. *FEMS Microbiol Rev*. 2020;44(6):684–700. doi:10.1093/femsre/fuaa017
31. Seidelman JL, Mantyh CR, Anderson DJ. Surgical Site Infection Prevention: a Review. *JAMA*. 2023;329(3):244–252. doi:10.1001/jama.2022.24075
32. WHO Guidelines Approved by the Guidelines Review Committee. *Global Guidelines for the Prevention of Surgical Site Infection*. Geneva: World Health Organization© World Health Organization 2018; 2018.
33. Kelishomi FZ, Nikkhahi F, Amereh S, et al. Evaluation of the therapeutic effect of a novel bacteriophage in the healing process of infected wounds with *Klebsiella pneumoniae* in mice. *J Glob Antimicrob Resist*. 2024;36:371–378. doi:10.1016/j.jgar.2024.01.018
34. Kumari S, Harjai K, Chhibber S. Evidence to support the therapeutic potential of bacteriophage Kpn5 in burn wound infection caused by *Klebsiella pneumoniae* in BALB/c mice. *J Microbiol Biotechnol*. 2010;20(5):935–941. doi:10.4014/jmb.0909.09010
35. Kifelew LG, Warner MS, Morales S, et al. Efficacy of phage cocktail AB-SA01 therapy in diabetic mouse wound infections caused by multidrug-resistant *Staphylococcus aureus*. *BMC Microbiol*. 2020;20(1):204. doi:10.1186/s12866-020-01891-8
36. Brisse S, Passet V, Haugaard AB, et al. wzi Gene sequencing, a rapid method for determination of capsular type for *Klebsiella* strains. *J Clin Microbiol*. 2013;51(12):4073–4078. doi:10.1128/JCM.01924-13
37. Mahony J, Kot W, Murphy J, et al. Investigation of the relationship between lactococcal host cell wall polysaccharide genotype and 936 phage receptor binding protein phylogeny. *Appl Environ Microbiol*. 2013;79(14):4385–4392. doi:10.1128/AEM.00653-13
38. Coil D, Jospin G, Darling AE. A5-miseq: an updated pipeline to assemble microbial genomes from Illumina MiSeq data. *Bioinformatics*. 2015;31(4):587–589. doi:10.1093/bioinformatics/btu661
39. Bankevich A, Nurk S, Antipov D, et al. SPAdes: a new genome assembly algorithm and its applications to single-cell sequencing. *J Comput Biol*. 2012;19(5):455–477. doi:10.1089/cmb.2012.0021
40. Schattner P, Brooks AN, Lowe TM. The tRNAscan-SE, snoscan and snoGPS web servers for the detection of tRNAs and snoRNAs. *Nucleic Acids Res*. 2005;33(Web Server issue):W686–9. doi:10.1093/nar/gki366
41. Kleinheinz KA, Joensen KG, Larsen MV. Applying the ResFinder and VirulenceFinder web-services for easy identification of acquired antibiotic resistance and *E. coli* virulence genes in bacteriophage and prophage nucleotide sequences. *Bacteriophage*. 2014;4(1):e27943. doi:10.4161/bact.27943
42. Tamura K, Stecher G, Kumar S. MEGA11: molecular evolutionary genetics analysis Version 11. *Mol Biol Evol*. 2021;38(7):3022–3027. doi:10.1093/molbev/msab120
43. Alikhan NF, Petty NK, Ben Zakour NL, et al. BLAST Ring Image Generator (BRIG): simple prokaryote genome comparisons. *BMC Genomics*. 2011;12:402. doi:10.1186/1471-2164-12-402
44. Li F, Tian F, Nazir A, et al. Isolation and genomic characterization of a novel Autographiviridae bacteriophage IME184 with lytic activity against *Klebsiella pneumoniae*. *Virus Res*. 2022;319:198873. doi:10.1016/j.virusres.2022.198873
45. Tang M, Huang Z, Zhang X, et al. Phage resistance formation and fitness costs of hypervirulent *Klebsiella pneumoniae* mediated by K2 capsule-specific phage and the corresponding mechanisms. *Front Microbiol*. 2023;14:1156292. doi:10.3389/fmicb.2023.1156292
46. Wang WX, Wu JZ, Zhang BL, et al. Phage therapy combats pan drug-resistant *Acinetobacter baumannii* infection safely and efficiently. *Int J Antimicrob Agents*. 2024;64(2):107220. doi:10.1016/j.ijantimicag.2024.107220
47. Archer NK, Wang Y, Ortines RV, et al. Preclinical models and methodologies for monitoring *Staphylococcus aureus* infections using noninvasive optical imaging. *Methods mol Biol*. 2020;2069:197–228.
48. Catalán-Nájera JC, Garza-Ramos U, Barrios-Camacho H. Hypervirulence and hypermucoviscosity: two different but complementary *Klebsiella* spp. phenotypes? *Virulence*. 2017;8(7):1111–1123. doi:10.1080/21505594.2017.1317412
49. Morales-León F, Matus-Köhler M, Araya-Vega P, et al. Molecular characterization of the convergent carbapenem-resistant and hypervirulent *Klebsiella pneumoniae* Strain K1-ST23, collected in Chile during the COVID-19 Pandemic. *Microbiol Spectr*. 2023;11(3):e0054023. doi:10.1128/spectrum.00540-23
50. Lin TL, Hsieh PF, Huang YT, et al. Isolation of a bacteriophage and its depolymerase specific for K1 capsule of *Klebsiella pneumoniae*: implication in typing and treatment. *J Infect Dis*. 2014;210(11):1734–1744. doi:10.1093/infdis/jiu332
51. Han P, Lin W, Fan H, Tong Y. Characterization of phage evolution and phage resistance in drug-resistant *Stenotrophomonas maltophilia*. *J Virol*. 2024;98(2):e0124923. doi:10.1128/jvi.01249-23
52. Majkowska-Skrobek G, Markwitz P, Sosnowska E, et al. The evolutionary trade-offs in phage-resistant *Klebsiella pneumoniae* entail cross-phage sensitization and loss of multidrug resistance. *Environ Microbiol*. 2021;23(12):7723–7740. doi:10.1111/1462-2920.15476
53. Ahmed HA, Ibrahim EHS, Abdelhaliem E, et al. Biotyping, virulotyping and biofilm formation ability of ESBL-*Klebsiella pneumoniae* isolates from nosocomial infections. *J Appl Microbiol*. 2022;132(6):4555–4568. doi:10.1111/jam.15563
54. Rojas D, Marcoleta AE, Gálvez-Silva M, et al. Inorganic polyphosphate affects biofilm assembly, capsule formation, and virulence of hypervirulent ST23 *Klebsiella pneumoniae*. *ACS Infect Dis*. 2024;10(2):606–623. doi:10.1021/acsinfecdis.3c00509
55. Hu Q, Huang L, Yang Y, et al. Essential phage component induces resistance of bacterial community. *Sci Adv*. 2024;10(36):eadp5057. doi:10.1126/sciadv.adp5057
56. Lakoh S, Yi L, Sevalie S, et al. Incidence and risk factors of surgical site infections and related antibiotic resistance in Freetown, Sierra Leone: a prospective cohort study. *Antimicrob Resist Infect Control*. 2022;11(1):39. doi:10.1186/s13756-022-01078-y
57. Billoro BB, Nunemo MH, Gelan SE. Evaluation of antimicrobial prophylaxis use and rate of surgical site infection in surgical ward of Wachemo University Nigist Eleni Mohammed Memorial Hospital, Southern Ethiopia: prospective cohort study. *BMC Infect Dis*. 2019;19(1):298. doi:10.1186/s12879-019-3895-5
58. Fish DN, Chow AT. The clinical pharmacokinetics of levofloxacin. *Clin Pharmacokinet*. 1997;32(2):101–119. doi:10.2165/00003088-199732020-00002
59. Giordano P, Weber K, Gesin G, et al. Skin and skin structure infections: treatment with newer generation fluoroquinolones. *Ther Clin Risk Manag*. 2007;3(2):309–317. doi:10.2147/tcrm.2007.3.2.309